

$Z^+(4430)$ and analogous heavy flavor statesGui-Jun Ding,¹ Wei Huang,¹ Jia-Feng Liu,¹ and Mu-Lin Yan^{1,2}¹*Department of Modern Physics, University of Science and Technology of China, Hefei, Anhui 230026, China*²*Interdisciplinary Center for Theoretical Study, University of Science and Technology of China, Hefei, Anhui 230026, China*

(Received 30 May 2008; published 23 February 2009)

The proximity of $Z^+(4430)$ to the $D^*\bar{D}_1$ threshold suggests that it may be a $D^*\bar{D}_1$ molecular state. The $D^*\bar{D}_1$ system has been studied dynamically from quark model, and state mixing effect is taken into account by solving the multichannel Schrödinger equation numerically. We suggest the most favorable quantum number is $J^P = 0^-$, if future experiments confirm $Z^+(4430)$ as a loosely bound molecule state. More precise measurements of $Z^+(4430)$ mass and width, partial wave analysis are helpful to understand its structure. The analogous heavy flavor mesons Z_{bb}^+ and Z_{bc}^{++} are studied as well, and the masses predicted in our model are in agreement with the predictions from potential model and QCD sum rule. We further apply our model to the $D\bar{D}^*$ and DD^* system. We find the exotic DD^* bound molecule does not exist, while the $1^{++} D\bar{D}^*$ bound state solution can be found only if the screening mass μ is smaller than 0.17 GeV. The state mixing effect between the molecular state and the conventional charmonium should be considered to understand the nature of $X(3872)$.

DOI: 10.1103/PhysRevD.79.034026

PACS numbers: 12.39.Jh, 12.40.Yx, 13.75.Lb

I. INTRODUCTION

In the past years many new mesons have been discovered through B meson decays. Recently, the Belle Collaboration has reported a narrow peak in the $\pi^+\psi'$ invariant mass spectrum in $B \rightarrow K\pi^\pm\psi'$ with statistical significance greater than 7σ [1]. This structure is denoted as $Z^+(4430)$. The Breit Wigner fit for this resonance yields the peak mass $M = 4433 \pm 4(\text{stat}) \pm 1(\text{syst})$ MeV and the width $\Gamma = 44_{-13}^{+17}(\text{stat})_{-11}^{+30}(\text{syst})$ MeV. The product branching fraction is determined to be $\mathcal{B}(B \rightarrow KZ^+(4430)) \cdot \mathcal{B}(Z^+(4430) \rightarrow \pi^+\psi') = (4.1 \pm 1.0(\text{stat}) \pm 1.3(\text{syst})) \times 10^{-5}$. Since the G parity of both π^+ and ψ' is negative, $Z^+(4430)$ is an isovector with positive G parity. However, $Z^+(4430)$ is far from being established, no significant evidence for $Z^-(4430)$ has been observed either in the total $J/\psi\pi^-$ or $\psi(2S)\pi^-$ mass distribution by the BABAR Collaboration [2].

There are already many theoretical investigations for the possible structures and the properties of $Z^+(4430)$ [3–18]. Because it is very close to the threshold of $D^*\bar{D}_1(2420)$, and the width of $Z^+(4430)$ is approximately the same as that of $D_1(2420)$, it is suggested that $Z^+(4430)$ could be a $D^*\bar{D}_1(2420)$ molecular state [3,4,6,11,16]. Other interpretations such as a tetraquark state [5,8] or a cusp in the $D^*\bar{D}_1$ channel [14] are proposed as well. In Ref. [3], we suggested how to distinguish the molecule and the tetraquark hypothesis, and $Z^+(4430)$ as a $D^*\bar{D}_1$ molecule was studied from the effective field theory. In Refs. [11,16], the authors investigated dynamically whether $Z^+(4430)$ could be a S wave $D^*\bar{D}_1$ or $D^*\bar{D}'_1$ molecular state by one-pion exchange and σ exchange.

In principle, nothing in QCD prevents the formation of nuclear-like bound states of mesons and speculation on the existence of such states dates back 30 years [19]. Törnqvist

suggested that two open flavor heavy mesons can form deuteron-like states due to the strong π exchange interaction [20], and the monopole form factor is introduced to regularize the interaction potential at short distance. In Ref. [21], the author investigated the possible heavy flavor molecules base on the long distance one-pion exchange and short distance quark interchange model. However, the dynamics of hadronic molecule is still unclear so far. In this work, we will dynamically study $Z^+(4430)$ and analogous heavy flavor states Z_{bb}^+ and Z_{bc}^{++} from the quark model. We shall discuss the interaction between two hadrons at the quark level instead of at the hadron level. The effective interactions between quarks including the screened color Coulomb, screened linear confinement, and spin-spin interactions are employed to describe the interactions between the components of the interacting hadrons.

This paper is organized as follows. In Sec. II, the canonical coordinate system and the effective interactions are introduced. We give the details of the evaluation of the matrix element in Sec. III. In sSec. IV, the $D^*\bar{D}_1$ system coupled with $D^*\bar{D}_2$ is studied, and the possible structure of $Z^+(4430)$ is discussed. In Sec. V, the analogous heavy flavor states Z_{bb}^+ and Z_{bc}^{++} , $D\bar{D}^*$ and DD^* systems are investigated, the static properties such as the mass and the root of mean square radius, etc. are calculated. We present our conclusions and some relevant discussions in Sec. VI. Finally, the spatial matrix elements involved are given in the appendix.

II. CANONICAL COORDINATE SYSTEM AND THE EFFECTIVE INTERACTIONS

The coordinate shown in Fig. 1 is taken as the canonical coordinate system, which defines the asymptotic states. The relevant coordinates of this system can be expressed

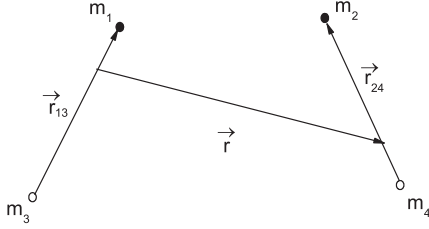


FIG. 1. Canonical coordinate system for the four quark system, where the black circle denotes the quark and the empty circle denotes the antiquark.

in terms of \mathbf{r}_{13} , \mathbf{r}_{24} , and \mathbf{r} as follows:

$$\begin{aligned}\mathbf{r}_{12} &= \frac{m_3}{m_1 + m_3} \mathbf{r}_{13} - \frac{m_4}{m_2 + m_4} \mathbf{r}_{24} - \mathbf{r} \\ \mathbf{r}_{14} &= \frac{m_3}{m_1 + m_3} \mathbf{r}_{13} + \frac{m_2}{m_2 + m_4} \mathbf{r}_{24} - \mathbf{r} \\ \mathbf{r}_{32} &= -\frac{m_1}{m_1 + m_3} \mathbf{r}_{13} - \frac{m_4}{m_2 + m_4} \mathbf{r}_{24} - \mathbf{r} \\ \mathbf{r}_{34} &= -\frac{m_1}{m_1 + m_3} \mathbf{r}_{13} + \frac{m_2}{m_2 + m_4} \mathbf{r}_{24} - \mathbf{r},\end{aligned}\quad (1)$$

where m_1 , m_2 , m_3 , and m_4 are, respectively, the masses of constituents 1, 2, 3, and 4. The relative position \mathbf{r} between the center of mass of the two mesons is

$$\mathbf{r} = -\frac{m_1 m_2 \mathbf{r}_{12} + m_1 m_4 \mathbf{r}_{14} + m_2 m_3 \mathbf{r}_{32} + m_3 m_4 \mathbf{r}_{34}}{(m_1 + m_3)(m_2 + m_4)}.\quad (2)$$

As is shown in Eq. (1), we can compactly represent the coordinate \mathbf{r}_{ij} in terms of \mathbf{r}_{13} , \mathbf{r}_{24} , and \mathbf{r} as follows:

$$\begin{aligned}\mathbf{r}_{ij} &= f_A(ij) \mathbf{r}_{13} + f_B(ij) \mathbf{r}_{24} - \mathbf{r}, \\ i &\in A \quad \text{and} \quad j \in B.\end{aligned}\quad (3)$$

The parameters $f_A(ij)$ and $f_B(ij)$ are listed in Table I.

In the above canonical coordinate, the Hamiltonian for this system, including the relative motion and the interaction between two mesons, is split into

$$H = H_0(A(13)) + H_0(B(24)) - \frac{1}{2\mu_{AB}} \nabla_{\mathbf{r}}^2 + V_I, \quad (4)$$

where $H_0(A(13))$ and $H_0(B(24))$ are, respectively, the Hamiltonian for the two mesons A and B , which contains the kinetic term and all the interactions within each meson.

TABLE I. The values for the parameters $f_A(ij)$ and $f_B(ij)$.

	$f_A(ij)$	$f_B(ij)$
$i = 1, j = 2$	$\frac{m_3}{m_1 + m_3}$	$-\frac{m_4}{m_2 + m_4}$
$i = 1, j = 4$	$\frac{m_3}{m_1 + m_3}$	$\frac{m_2}{m_2 + m_4}$
$i = 3, j = 2$	$-\frac{m_1}{m_1 + m_3}$	$-\frac{m_4}{m_2 + m_4}$
$i = 3, j = 4$	$-\frac{m_1}{m_1 + m_3}$	$\frac{m_2}{m_2 + m_4}$

μ_{AB} is the reduced mass $\mu_{AB} = \frac{M_A M_B}{M_A + M_B}$. The third term $-\frac{1}{2\mu_{AB}} \nabla_{\mathbf{r}}^2$ is the kinetic energy operator of the relative motion. The interaction potential V_I is the sum of two-body interaction between quarks in the mesons A and B ,

$$V_I = \sum_{i \in A, j \in B} V_{ij}(r_{ij}). \quad (5)$$

The phenomenological interaction between a quark and an antiquark in a single meson (e.g. A and B) is reasonably well known, and it is described by the short distance one-gluon exchange interaction and the long distance phenomenological confinement interaction [22,23]

$$V_{ij}^{\text{phe}}(\mathbf{r}_{ij}) = \frac{\lambda(i)}{2} \cdot \frac{\lambda(j)}{2} \left[\frac{\alpha_s}{r_{ij}} - \frac{3b}{4} r_{ij} - \frac{8\pi\alpha_s}{3m_i m_j} \delta^3(\mathbf{r}_{ij}) \mathbf{s}_i \cdot \mathbf{s}_j \right], \quad (6)$$

where α_s is the strong coupling constant, b is the string tension, m_i , and m_j are the masses of the interacting constituents. For an antiquark, the generator $\lambda/2$ is replaced by $-\lambda^T/2$.

Since we mainly concentrate on the molecular states comprising two heavy flavor mesons in this work, and the molecule is generally weakly bound. Therefore, the separation between the two mesons in the molecule is rather larger than the average radius of the individual meson, and the two mesons interact mainly through two gluons exchange processes [24,25], which results in the color van der Waals interaction. By comparing with the van der Waals interaction between electric dipoles in QED, the author in Ref. [26] introduced the effective charges for quarks and antiquarks to describe the color van der Waals interaction between two mesons. The effective charges for quark and antiquark, respectively, are $C_q = \sqrt{\frac{N_c^2 - 1}{2N_c}}$ and $C_{\bar{q}} = -\sqrt{\frac{N_c^2 - 1}{2N_c}}$, and here N_c is the number of color with $N_c = 3$ in QCD. It is remarkable that the effective charge correctly describes the interaction between quark and antiquark in an individual meson as well. The effective charge is also consistent with the Lattice QCD results, which found the nonperturbative potential between a quark and an antiquark in different representations is proportional to the eigenvalue of the quadratic Casimir operator [27].

Different from the interactions between quarks in a single meson, as the interaction between the constituents in a molecule takes place at large distances, we are well advised to use a screened potential to represent the effects of dynamical quarks and gluon [28]. A simple way to incorporate the screening effect is to replace \mathbf{k}^2 in the Fourier transformation of the interaction potential by $\mathbf{k}^2 + \mu^2$ [26,29], where μ is the screening mass. With the effective charge and the screening effect in mind, in momentum space, the effective interaction potential $V_{ij}^{\text{eff}}(\mathbf{k})$ between two quarks in the mesons A and B is

$$V_{ij}^{\text{eff}}(\mathbf{k}) = C_i C_j \left[\frac{4\pi\alpha_s}{\mathbf{k}^2 + \mu^2} + \frac{6\pi b}{(\mathbf{k}^2 + \mu^2)^2} - \frac{8\pi\alpha_s}{3m_i m_j} \mathbf{s}_i \cdot \mathbf{s}_j \right]. \quad (7)$$

The effective interaction in coordinate space $V_{ij}^{\text{eff}}(\mathbf{r}_{ij})$ is the Fourier transformation of $V_{ij}^{\text{eff}}(\mathbf{k})$

$$V_{ij}^{\text{eff}}(\mathbf{r}_{ij}) = \int \frac{d^3\mathbf{k}}{(2\pi)^3} e^{i\mathbf{k}\cdot\mathbf{r}_{ij}} V_{ij}^{\text{eff}}(\mathbf{k}). \quad (8)$$

Therefore, in coordinate space the effective interaction $V_{ij}^{\text{eff}}(\mathbf{r}_{ij})$ is

$$V_{ij}^{\text{eff}}(\mathbf{r}_{ij}) = C_i C_j \left[\frac{\alpha_s e^{-\mu r_{ij}}}{r_{ij}} + \frac{3b}{4\mu} e^{-\mu r_{ij}} - \frac{8\pi\alpha_s}{3m_i m_j} \delta^3(\mathbf{r}_{ij}) \mathbf{s}_i \cdot \mathbf{s}_j \right]. \quad (9)$$

In this work, we will use the above effective interaction $V_{ij}^{\text{eff}}(\mathbf{r}_{ij})$ to study the possible heavy flavor molecules dynamically. Comparing with Ref. [26], we have introduced the spin-spin interaction in addition to the screened color Coulomb and the screened linear confinement interactions. In the light quark hadrons, the spin-spin hyperfine interaction makes the dominant contribution to the hadron-hadron interactions [30]. Whereas, for the heavy flavor mesons, the hyperfine interaction contribution is smaller due to the large heavy quark mass [31,32]. Therefore, we expect that the contribution of spin-spin interaction should be smaller than those of the screened color Coulomb and screened linear confinement interactions. However, the spin-spin hyperfine interaction may play an important role when we study the dynamics of molecular state, since the binding energy of molecular state is usually rather small. On the other hand, if we neglect the spin-spin interaction, the static properties of the molecule, such as the binding energy and the root of mean square radius (rms), etc., would be independent of the spin of the molecular state, which contradict with the experimental observations for deuteron.

As a result of the residual interaction V_I between two mesons, at short distance the mesons may excite as they interact, and they could be virtually whatever the dynamics requires. This means that we need to consider the state mixing effect. It has been shown that the state mixing effect plays an important role in obtaining the phenomenologically required potential, when we study the nucleon-nucleon and nucleon-antinucleon interactions from the chiral soliton model [33,34]. The eigenvalue equation for the system is

$$(H - E)|\Psi\rangle = 0, \quad (10)$$

where E and $|\Psi\rangle$ are, respectively, the eigenvalue and the corresponding eigenfunction. If there is no residual interactions V_I between A and B , the eigenfunction of the total system would simply be the product of A meson's wave-

function and B meson's. Consequently, it is natural to expand the eigenfunction $|\Psi\rangle$ in terms of the model wavefunctions

$$|\Psi\rangle = \sum_{\alpha'} \psi(\mathbf{r})_{\alpha'} |\Phi_{\alpha'}(A, B)\rangle, \quad (11)$$

where $\psi(\mathbf{r})_{\alpha}$ is the relative wavefunction between the mesons A and B , and $|\Phi_{\alpha}(A, B)\rangle = |\Phi_A\rangle |\Phi_B\rangle$ denotes the intrinsic state of the two mesons, which will be mixed under the interaction V_I . The wavefunction $|\Phi_A\rangle$ satisfies the Schrödinger equation $(H_0(A(13)) - M_A)|\Phi_A\rangle = 0$, where $|\Phi_A\rangle$ depends on the relative coordinate \mathbf{r}_{13} , and similarly for $|\Phi_B\rangle$. Inserting wavefunction $|\Psi\rangle$ into the eigenequation Eq. (10), multiplying by $\langle\Phi_{\alpha}|$ and integrating over the internal coordinates, we obtain

$$\begin{aligned} & \left(-\frac{1}{2\mu_{AB}} \nabla_{\mathbf{r}}^2 + V_{I\alpha\alpha}(\mathbf{r}) + E_{\alpha} - E \right) \psi_{\alpha}(\mathbf{r}) \\ & = - \sum_{\alpha' \neq \alpha} V_{I\alpha\alpha'}(\mathbf{r}) \psi_{\alpha'}(\mathbf{r}), \end{aligned} \quad (12)$$

where $E_{\alpha} = M_A + M_B$ is the energy eigenvalue of channel α , $V_{I\alpha\alpha'}(\mathbf{r}) = \langle\Phi_{\alpha}|V_I|\Phi_{\alpha'}\rangle$ is the matrix element of the interaction potential V_I , it is a function of the relative coordinate \mathbf{r} , the intrinsic coordinates \mathbf{r}_{13} and \mathbf{r}_{24} have been integrated out. There is clearly one equation for each state α , and they are coupled each other by the terms on the right-hand side. It is important to note that all the transitions represented by the right-hand of Eq. (12) contribute coherently. If $|E_{\alpha} - E_{\alpha'}| \gg |V_{I\alpha\alpha'}(\mathbf{r})|$ with $\alpha \neq \alpha'$, then the coupled channel Schrödinger equation Eq. (12) is reduced to the single channel Schrödinger equation

$$\left(-\frac{1}{2\mu_{AB}} \nabla_{\mathbf{r}}^2 + V'_{I\alpha\alpha}(\mathbf{r}) + E_{\alpha} - E \right) \psi_{\alpha}(\mathbf{r}) = 0, \quad (13)$$

where $V'_{I\alpha\alpha}(\mathbf{r})$ is the effective interaction potential

$$V'_{I\alpha\alpha}(\mathbf{r}) = V_{I\alpha\alpha}(\mathbf{r}) - \sum_{\alpha' \neq \alpha} \frac{|V_{I\alpha\alpha'}(\mathbf{r})|^2}{E_{\alpha'} - E_{\alpha}}. \quad (14)$$

Equations (13) and (14) are exactly the results of the second order perturbation theory to deal with the state mixing effect, and this simplification is widely used [26,33,34]. However, if $|E_{\alpha} - E_{\alpha'}|$ is rather small or of the same order comparing with $|V_{I\alpha\alpha'}(\mathbf{r})|$, we have to solve the coupled channel Schrödinger equation exactly. Although in principle we should solve the infinite set of equations implied by Eq. (12), in practice we only need to concentrate on the nearly degenerate channels, which is a good approximation.

III. EVALUATION OF THE MATRIX ELEMENT

$$V_{I\alpha\alpha'}(\mathbf{r})$$

For a system consisting of two mesons A and B with total angular momentum J and the third component J_z , its

wavefunction is written as

$$\begin{aligned} |\Phi_{\alpha}^{J,J_z}(A, B)\rangle &= \sum_{S,L} [(\chi_A \chi_B)^S (\psi_A \psi_B)^L]^{J,J_z} [(\chi_A \psi_A)^{J_A} (\chi_B \psi_B)^{J_B}]^{J,J_z} [(\chi_A \chi_B)^S (\psi_A \psi_B)^L]^{J,J_z} \\ &= \sum_{S,S_z,L} \hat{S} \hat{L} \hat{J}_A \hat{J}_B \begin{Bmatrix} S_A & S_B & S \\ L_A & L_B & L \\ J_A & J_B & J \end{Bmatrix} \langle S, S_z; L, J_z - S_z | J, J_z \rangle (\chi_A \chi_B)^{S,S_z} |(\psi_A \psi_B)^{L,J_z - S_z}\rangle, \end{aligned} \quad (15)$$

where $\hat{S} = \sqrt{2S+1}$, χ is the spin wavefunction, and ψ represents the spatial wavefunction. S_A, L_A and J_A denote, respectively, the spin, the orbital angular momentum, and the total angular momentum of meson A with similar notations for the meson B . From Eqs. (5) and (9), it is obvious that each term of V_I can be factorized into the spatial and spin relevant part; consequently, the interaction potential V_I can be rewritten as

$$V_I = \sum_{i \in A, j \in B} \sum_{k=1}^3 C_i C_j V_r^{(k)}(r_{ij}) V_s^{(k)}, \quad (16)$$

where the superscript (k) represents, respectively, the screened color Coulomb, screened linear, and spin-spin interactions for $k = 1, 2, 3$. Concretely, $V_s^{(1)} = V_s^{(2)} = 1$, $V_s^{(3)} = \mathbf{s}_i \cdot \mathbf{s}_j$, and the spatial part $V_r^{(k)}(r_{ij})$ can be read from Eq. (9) straightforwardly. Therefore, the matrix element $V_{I\alpha\alpha'}(\mathbf{r})$ is the sum of 12 terms, and each term is of the form

$$\begin{aligned} \langle \Phi_{\alpha'}^{J',J'_z} | V_r^{(k)} V_s^{(k)} | \Phi_{\alpha}^{J,J_z} \rangle &= \sum_{S,S_z,L,S',S'_z,L'} \hat{S} \hat{L} \hat{J}_A \hat{J}_B \hat{S}' \hat{L}' \hat{J}_{A'} \hat{J}_{B'} \begin{Bmatrix} S_A & S_B & S \\ L_A & L_B & L \\ J_A & J_B & J \end{Bmatrix} \begin{Bmatrix} S_{A'} & S_{B'} & S' \\ L_{A'} & L_{B'} & L' \\ J_{A'} & J_{B'} & J' \end{Bmatrix} \langle S, S_z; L, J_z - S_z | J, J_z \rangle \\ &\times \langle S', S'_z; L', J'_z - S'_z | J', J'_z \rangle \langle (\psi_{A'} \psi_{B'})^{L',J'_z - S'_z} | V_r^{(k)} | (\psi_A \psi_B)^{L,J_z - S_z} \rangle \langle (\chi_{A'} \chi_{B'})^{S',S'_z} | V_s^{(k)} | (\chi_A \chi_B)^{S,S_z} \rangle. \end{aligned} \quad (17)$$

It is obvious that both the spatial matrix element $\langle (\psi_{A'} \psi_{B'})^{L',J'_z - S'_z} | V_r^{(k)} | (\psi_A \psi_B)^{L,J_z - S_z} \rangle$ and the spin matrix element $\langle (\chi_{A'} \chi_{B'})^{S',S'_z} | V_s^{(k)} | (\chi_A \chi_B)^{S,S_z} \rangle$ are needed. Firstly, we consider the spatial matrix element

$$\begin{aligned} \langle (\psi_{A'} \psi_{B'})^{L',J'_z - S'_z} | V_r^{(k)}(r_{ij}) | (\psi_A \psi_B)^{L,J_z - S_z} \rangle &= \sum_{L_{Az}, L_{Bz}, L_{A'z}, L_{B'z}} \langle L_{A'}, L_{A'z}; L_{B'}, L_{B'z} | L', J'_z - S'_z \rangle \langle L_A, L_{Az}; L_B, L_{Bz} | L, J_z - S_z \rangle \\ &\times \langle \psi_{A'}^{L_{A'}, L_{A'z}}(\mathbf{r}_{13}) \psi_{B'}^{L_{B'}, L_{B'z}}(\mathbf{r}_{24}) | V_r^{(k)}(r_{ij}) | \psi_A^{L_A, L_{Az}}(\mathbf{r}_{13}) \psi_B^{L_B, L_{Bz}}(\mathbf{r}_{24}) \rangle, \end{aligned} \quad (18)$$

where

$$\begin{aligned} \langle \psi_{A'}^{L_{A'}, L_{A'z}}(\mathbf{r}_{13}) \psi_{B'}^{L_{B'}, L_{B'z}}(\mathbf{r}_{24}) | V_r^{(k)}(r_{ij}) | \psi_A^{L_A, L_{Az}}(\mathbf{r}_{13}) \psi_B^{L_B, L_{Bz}}(\mathbf{r}_{24}) \rangle &\equiv \langle L_{A'}, L_{A'z}; L_{B'}, L_{B'z} | V_r^{(k)}(r_{ij}) | L_A, L_{Az}; L_B, L_{Bz} \rangle \\ &= \int d^3 \mathbf{r}_{13} \int d^3 \mathbf{r}_{24} (\psi_{A'}^{L_{A'}, L_{A'z}}(\mathbf{r}_{13}))^* (\psi_{B'}^{L_{B'}, L_{B'z}}(\mathbf{r}_{24}))^* \psi_A^{L_A, L_{Az}}(\mathbf{r}_{13}) \psi_B^{L_B, L_{Bz}}(\mathbf{r}_{24}) V_r^{(k)}(f_A(ij)\mathbf{r}_{13} + f_B(ij)\mathbf{r}_{24} - \mathbf{r}). \end{aligned} \quad (19)$$

In this work, the spatial wavefunctions are taken as the simple harmonic oscillator wavefunctions, which is a widely used approximation in the quark model calculations. The integral in Eq. (19) can be evaluated analytically in coordinate space following the procedures in Ref. [35]. On the other hand, this integration can be performed in momentum space as well, then the calculation will be greatly simplified [26,32],

$$\langle L_{A'}, L_{A'z}; L_{B'}, L_{B'z} | V_r^{(k)}(r_{ij}) | L_A, L_{Az}; L_B, L_{Bz} \rangle = \int \frac{d^3 \mathbf{p}}{(2\pi)^3} e^{-i\mathbf{p} \cdot \mathbf{r}} \rho_{L_{A'}, L_{A'z}; L_A, L_{Az}}[f_A(ij)\mathbf{p}] \rho_{L_{B'}, L_{B'z}; L_B, L_{Bz}}[f_B(ij)\mathbf{p}] V^{(k)}(\mathbf{p}), \quad (20)$$

where

$$\rho_{L_{A'}, L_{A'z}; L_A, L_{Az}}(\mathbf{p}) = \int d^3 \mathbf{r}_{13} e^{i\mathbf{p} \cdot \mathbf{r}_{13}} (\psi_{A'}^{L_{A'}, L_{A'z}}(\mathbf{r}_{13}))^* \psi_A^{L_A, L_{Az}}(\mathbf{r}_{13}) V^{(k)}(\mathbf{p}) = \int d^3 \mathbf{r}_{ij} e^{-i\mathbf{p} \cdot \mathbf{r}_{ij}} V_r^{(k)}(\mathbf{r}_{ij}). \quad (21)$$

Note that $V^{(k)}(\mathbf{p})$ can be read from Eq. (7) directly. For the given quantum numbers L_A, L_{Az} , etc., the above integral can be

straightforwardly calculated although it is somewhat lengthy, and the matrix elements involved in our calculation are listed in the appendix.

Next we turn to the spin matrix element $\langle(\chi_{A'}\chi_{B'})^{S',S'_z}|V_s^{(k)}|(\chi_A\chi_B)^{S,S_z}\rangle$. We denote the spin of the constituents 1, 2, 3, and 4 by s_1, s_2, s_3 , and s_4 , respectively. In the present work, the constituent is quark or antiquark; consequently, we have $s_1 = s_2 = s_3 = s_4 = \frac{1}{2}$. We would like to recouple the constituents so that the spin operator $V_s^{(k)}$ ($k = 1, 2, 3$) matrix elements can be easily calculated. We have

$$\begin{aligned} |(\chi_A\chi_B)^{S,S_z}\rangle &= [(s_1s_3)S_A(s_2s_4)S_B]^{S,S_z} = \sum_{S_{12},S_{34}} \hat{S}_{12}\hat{S}_{34}\hat{S}_A\hat{S}_B \begin{Bmatrix} s_1 & s_3 & S_A \\ s_2 & s_4 & S_B \\ S_{12} & S_{34} & S \end{Bmatrix} |[(s_1s_2)S_{12}(s_3s_4)S_{34}]^{S,S_z}\rangle \\ &= \sum_{S_{14},S_{32}} (-1)^{S_B-s_2-s_4} \hat{S}_{14}\hat{S}_{32}\hat{S}_A\hat{S}_B \begin{Bmatrix} s_1 & s_3 & S_A \\ s_4 & s_2 & S_B \\ S_{14} & S_{32} & S \end{Bmatrix} |[(s_1s_4)S_{14}(s_3s_2)S_{32}]^{S,S_z}\rangle. \end{aligned} \quad (22)$$

It is obvious that the matrix element of $V_s^{(1)} = V_s^{(2)} = \mathbf{1}$ is

$$\langle(\chi_{A'}\chi_{B'})^{S',S'_z}|V_s^{(1)}|(\chi_A\chi_B)^{S,S_z}\rangle = \langle(\chi_{A'}\chi_{B'})^{S',S'_z}|V_s^{(2)}|(\chi_A\chi_B)^{S,S_z}\rangle = \langle(\chi_{A'}\chi_{B'})^{S',S'_z}|\mathbf{1}|(\chi_A\chi_B)^{S,S_z}\rangle = \delta_{SS'}\delta_{S_zS'_z}\delta_{S_AS'_A}\delta_{S_BS'_B}. \quad (23)$$

The matrix element of $V_s^{(3)} = \mathbf{s}_i \cdot \mathbf{s}_j$ can be derived straightforwardly by using the recoupling formula Eq. (22). For $(i, j) = (1, 2)$ or $(3, 4)$, the matrix element is given by

$$\begin{aligned} \langle(\chi_{A'}\chi_{B'})^{S',S'_z}|V_s^{(3)}|(\chi_A\chi_B)^{S,S_z}\rangle &= \langle(\chi_{A'}\chi_{B'})^{S',S'_z}|\mathbf{s}_i \cdot \mathbf{s}_j|(\chi_A\chi_B)^{S,S_z}\rangle \\ &= \delta_{SS'}\delta_{S_zS'_z} \sum_{S_{12},S_{34}} \hat{S}_A\hat{S}_B\hat{S}_{A'}\hat{S}_{B'}\hat{S}_{12}^2\hat{S}_{34}^2 \begin{Bmatrix} s_1 & s_3 & S_{A'} \\ s_2 & s_4 & S_{B'} \\ S_{12} & S_{34} & S \end{Bmatrix} \begin{Bmatrix} s_1 & s_3 & S_A \\ s_2 & s_4 & S_B \\ S_{12} & S_{34} & S \end{Bmatrix} \frac{1}{2} \\ &\quad \times [S_{ij}(S_{ij} + 1) - s_i(s_i + 1) - s_j(s_j + 1)]. \end{aligned} \quad (24)$$

For $(i, j) = (1, 4)$ or $(3, 2)$, the matrix element of $V_s^{(3)} = \mathbf{s}_i \cdot \mathbf{s}_j$ is

$$\begin{aligned} \langle(\chi_{A'}\chi_{B'})^{S',S'_z}|V_s^{(3)}|(\chi_A\chi_B)^{S,S_z}\rangle &= \langle(\chi_{A'}\chi_{B'})^{S',S'_z}|\mathbf{s}_i \cdot \mathbf{s}_j|(\chi_A\chi_B)^{S,S_z}\rangle \\ &= \delta_{SS'}\delta_{S_zS'_z} \sum_{S_{14},S_{32}} (-1)^{S_{B'}+S_B} \hat{S}_A\hat{S}_B\hat{S}_{A'}\hat{S}_{B'}\hat{S}_{14}^2\hat{S}_{32}^2 \begin{Bmatrix} s_1 & s_3 & S_{A'} \\ s_4 & s_2 & S_{B'} \\ S_{14} & S_{32} & S \end{Bmatrix} \begin{Bmatrix} s_1 & s_3 & S_A \\ s_4 & s_2 & S_B \\ S_{14} & S_{32} & S \end{Bmatrix} \frac{1}{2} \\ &\quad \times [S_{ij}(S_{ij} + 1) - s_i(s_i + 1) - s_j(s_j + 1)]. \end{aligned} \quad (25)$$

IV. Z⁺(4430) AND D^{*}D₁ MOLECULAR STATE

Because the mass of Z⁺(4430) is close to the D^{*} \bar{D}_1 threshold and its width roughly is the same as that of D₁, it is very likely that Z⁺(4430) is a loosely bound D^{*} \bar{D}_1 molecular state. In this section we will dynamically study whether there exists a D^{*} \bar{D}_1 molecule state consistent with Z⁺(4430). Since $m_{D_1} \simeq 2.422$ GeV, $m_{D'_1} \simeq (2.441 \pm 0.032)$ GeV, and $m_{D_2} \simeq 2.459$ GeV [36], the masses of D^{*} \bar{D}_1 , D^{*} \bar{D}'_1 and D^{*} \bar{D}_2 are close to each other. Under the residual interaction V_I in Eqs. (5) and (9), these three channels would be coupled with each other. However, the width of D₁ is very large $\Gamma \sim 384$ MeV [36]; consequently, there should be very small D^{*} \bar{D}'_1 component in the molecular state, otherwise, it would decay so quickly

that a weakly bound molecule cannot form. As a result, we shall consider both D^{*} \bar{D}_1 and D^{*} \bar{D}_2 channels here, the effective interaction potential is induced by the pairwise interactions between quarks or antiquarks. Then we solve the corresponding two channels coupled Schrödinger equation to find whether there are bound state solutions, where we only concentrate on the lowest mass state.

The model parameters employed are $m_u = m_d = 0.334$ GeV, $m_c = 1.776$ GeV, $m_b = 5.102$ GeV, $b = 0.18$ GeV², which is a set of fairly conventional quark model parameters. In Ref. [26] the screening mass μ is taken to be 0.28 GeV, which was found to be consistent with the string breaking mechanism and meanwhile give a good description of the charmonium masses [37]. The uncertainty of screening parameter μ will be considered

in the following. Moreover, we use a running coupling constant $\alpha_s(Q^2)$, which is given by

$$\alpha_s(Q^2) = \frac{12\pi}{(33 - 2n_f) \ln(A + Q^2/B^2)}, \quad (26)$$

with $A = 10$ and $B = 0.31$ GeV. Theoretical estimates for the harmonic oscillator parameter β scatter in a relative large region 0.3–0.7 GeV. Many recent quark model studies of meson and baryon decays use a value of $\beta = 0.4$ GeV [38,39]; therefore, we assume $\beta_A = \beta_B = 0.4$ GeV in this work.

In the limit that the heavy quark mass becomes infinite, the properties of the meson are determined by the light quark. The light quark is characterized by their total angular momentum, $j_q = s_q + L$, where s_q is the light quark spin and L is its orbital angular momentum. The prime superscript (D'_1 or B'_1) is used for the state with $j_q = 1/2$ and is very broad. The unprimed state (D_1 or B_1) is used for the $j_q = 3/2$ state, and is rather narrow. Heavy-light mesons are not charge conjugation eigenstates and so mixing can occur among the states with the same J^P . The two $J = 1$ states D_1 and D'_1 are coherent superposition of the quark model 3P_1 and 1P_1 states

$$\begin{aligned} |D_1\rangle &= \cos\theta|^1P_1\rangle + \sin\theta|^3P_1\rangle \\ |D'_1\rangle &= -\sin\theta|^1P_1\rangle + \cos\theta|^3P_1\rangle. \end{aligned} \quad (27)$$

Little is known about the mixing angle θ at present. In the heavy quark limit, the mixing angle is predicted to be -54.7° or 35.3° if the expectation value of the heavy quark spin-orbit interaction is positive or negative [40]. Since the former implies that the 2^+ state mass is larger than that of the 0^+ state, and this agrees with the current experiment data, we shall employ $\theta = -54.7^\circ$ in the following. The above analysis applies to B_1 and B'_1 mixing as well.

There are various methods of integrating the multichannel Schrödinger equation numerically. In this work we shall employ two packages MATSCS [41] and FESSDE.2 [42] to perform the numerical calculations so that the results obtained by one program can be checked by another. The first package is a MATLAB software, and the second is written in FORTRAN 77. Both packages can quickly and accurately solve the eigenvalue problem for systems of the coupled Schrödinger equations, and the results obtained by two codes are exactly the same within error.

Calculating the relevant matrix elements of the residual interaction V_l following the methods outlined in Sec. III, then we solve the coupled channel Schrödinger equation numerically. The numerical results for the lowest energy states are listed in Table II. We find that the $J^P = 0^- D^* \bar{D}_1$ bound state can exist for reasonable screening mass μ . The binding energy is found to decrease with μ , since a smaller μ gives a stronger potential at short distance, which is displayed in Fig. 2. With $\mu = 0.28$ GeV and 0.33 GeV, the

TABLE II. The predictions about the mass, the rms and the ratio of $D^* \bar{D}_1$ probability to $D^* \bar{D}_2$ probability for the bound states of the $D^* \bar{D}_1$ and $D^* \bar{D}_2$ system.

	μ (GeV)	Mass (MeV)	r_{rms} (fm)	$P(D^* \bar{D}_1) : P(D^* \bar{D}_2)$ (%)
$J = 0$	0.23	4402.438	0.845	100:0
	0.28	4411.839	0.971	100:0
	0.33	4419.014	1.183	100:0
$J = 1$	0.16	4427.699	2.650	86.747:13.253
	0.23	not bounded	-	-
	0.28	not bounded	-	-
$J = 2$	0.23	4401.732	0.702	37.220:62.780
	0.28	4414.432	0.832	43.148:56.852
	0.33	4423.988	1.272	55.945:44.055

bound state mass is about 4411.839 MeV and 4419.014 MeV, respectively, and the root of mean square radius is 0.971 fm and 1.183 fm, respectively, which are widely extended in space. Because the total angular momentum of S wave $D^* \bar{D}_2$ is 1, 2, or 3, it cannot be 0. Hence, $D^* \bar{D}_1$ will not mix with $D^* \bar{D}_2$ for the $J^P = 0^-$ state, then we only need to solve the single channel Schrödinger equation in this case. Similar bound state solutions have been found for $J^P = 2^-$, and the binding energy is approximately the same as that of the $J^P = 0^-$ case for the same μ value. Both the 0^- and 2^- bound states are widely extended, it is a good feature of molecular states. The wavefunctions for the two states with $\mu = 0.28$ GeV are shown in Fig. 3. For the $J^P = 1^-$, bound state solutions could be found only if the screening mass μ is smaller than 0.16 GeV, which is quite different from the favored value 0.28 GeV. Therefore, we tend to conclude that the $1^- D^* \bar{D}_1$ molecule does not exist. In short, both 0^- and $2^- D^* \bar{D}_1$ bound states are predicted to exist in our model, whereas only the $0^- D^* \bar{D}_1$ molecule may exist in the π and σ

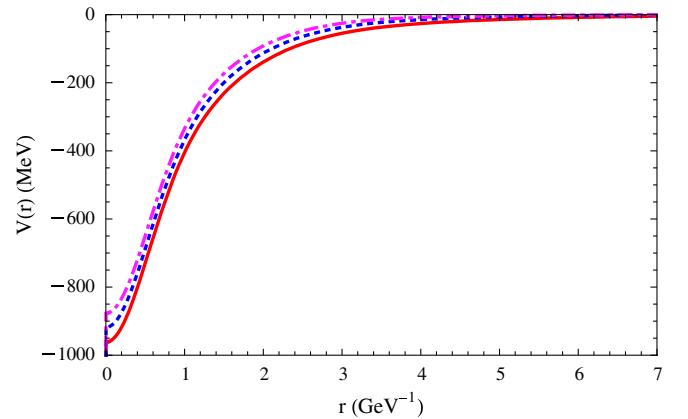


FIG. 2 (color online). The potential for $0^- D^* \bar{D}_1$ as a function of the separation r for different screening mass μ . The solid line, short dashed, and dashed-dotted lines represent the potentials for $\mu = 0.23$ GeV, 0.33 GeV, and 0.43 GeV, respectively.

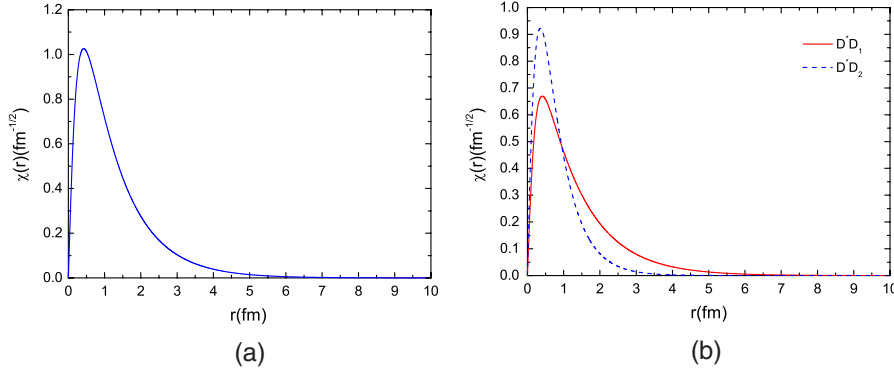


FIG. 3 (color online). The radial wave functions $\chi(r) = rR(r)$ for the possible bound states of the $D^*\bar{D}_1$ and $D^*\bar{D}_2$ system, (a) and (b), respectively, correspond to $J^P = 0^-$ and $J^P = 2^-$ states.

exchange model from the heavy quark effective theory [16].

Since the production of $Z^+(4430)$ is highly suppressed in B meson decay for $J^P = 2^-$, the quantum $J^P = 0^-$ is favored if future experiments confirm $Z^+(4430)$ as a loosely molecular state. Experimentally the mass and width of $Z^+(4430)$ are fitted to be $4433 \pm 4(\text{stat}) \pm 1(\text{syst})$ MeV and $44_{-13}^{+17}(\text{stat})_{-11}^{+30}(\text{syst})$ MeV, respectively. Considering the large error in the width measurement and the theoretical uncertainties from the screening mass μ , $Z^+(4430)$ as a $0^- D^*\bar{D}_1$ molecular state cannot be excluded. More precise measurements of its mass and width, partial wave analysis are important to understand the nature of $Z^+(4430)$. As is suggested in Ref. [14], it is highly desirable to use the full amplitude including both the production and the decay processes, in performing partial wave analysis to determine the spin parity of $Z^+(4430)$. If $J^P = 0^-$ or 2^- is favored by future partial wave analysis, the molecule hypothesis is strongly supported, otherwise it is not appropriate to interpret $Z^+(4430)$ as a $D^*\bar{D}_1$ molecule.

V. APPLICATION TO OTHER HEAVY FLAVOR SYSTEMS

In this section, we shall apply our model to the $1^{++} D\bar{D}^*$ system, the heavy flavor systems obtained by replacing the charm quark/antiquark in $Z^+(4430)$ with bottom quark/antiquark, and DD^* system, respectively. Possible molecular states and their static properties are studied in detail.

A. $1^{++} D\bar{D}^*$ and $X(3872)$

The narrow charmoniumlike state $X(3872)$ was discovered by the Belle Collaboration in the decay $B^+ \rightarrow K^+ + X(3872)$ followed by $X(3872) \rightarrow J/\psi \pi^+ \pi^-$ with a statistical significance of 10.3σ [43]. The existence of $X(3872)$ has been confirmed by the CDF [44], D0 [45], and BABAR

collaborations [46]. The CDF Collaboration measured the $X(3872)$ mass to be $(3871.61 \pm 0.16(\text{stat}) \pm 0.19(\text{sys.}))$ MeV. Its quantum number is strongly preferred to be 1^{++} [47]. $X(3872)$ was suggested to be a $D\bar{D}^*$ molecule [48], because it is very close to the $D\bar{D}^*$ threshold. Recently, several authors investigated whether a molecule corresponding to $X(3872)$ could be dynamically realizable [49–52]. Notably, Suzuki argued that the one-pion exchange forces are only able to make a feeble attraction at best. We shall dynamically study the $D\bar{D}^*$ system in our model. The $1^{++} D\bar{D}^*$ state would couple with $D_1\bar{D}_2$ under the pairwise residual interactions, we would like to point that the allowed quantum numbers of S wave $D^*\bar{D}^*$ are 0^{++} , 1^{+-} and 2^{++} . Solving the two channel coupled Schrödinger equation numerically, the numerical results are shown in Table III. We find the bound state solutions appear only if the screening mass μ is smaller than 0.17 GeV, with $\mu = 0.13$ GeV the bound state mass is 3870.489 MeV, and it is almost completely consisted of $D\bar{D}^*$. For a reasonable value of μ of around 0.28 GeV, we cannot find bound states. Consequently, $X(3872)$ as a $D\bar{D}^*$ molecule seems to be disfavored in our model. However, it is remarkable that the unexpectedly large branch ratio of $X(3872) \rightarrow \psi(2S)\gamma$ recently was reported [53], which indicates the mixing between the molecular state and the conventional charmonium state should be taken into account. This mixing effect may enhance the binding of the molecular component. This subject is so subtle that it is outside the scope of the present work.

TABLE III. The predictions for the mass, the rms and the ratio of $D\bar{D}^*$ probability to $D_1\bar{D}_2$ probability for the bound states of the $1^{++} D\bar{D}^*$ and $D_1\bar{D}_2$ system.

μ (GeV)	Mass (MeV)	r_{rms} (fm)	$P(D\bar{D}^*) : P(D_1\bar{D}_2)$
0.13	3870.489	2.964	99.966:0.034
0.23	not bounded	-	-
0.28	not bounded	-	-

TABLE IV. The predictions about the mass, the rms, the probabilities of the $B^*\bar{B}_1$ and $B^*\bar{B}_2$ components for Z_{bb}^+ . The mass predictions in Refs. [7,10] are shown as well.

	μ (GeV)	Mass (MeV) in [7]	Mass (MeV) in [10]	Mass (MeV)	r_{rms} (fm)	$P(B^*\bar{B}_1) : P(B^*\bar{B}_2)$ (%)
$J = 0$	0.23			10 865.468	0.309	100:0
				11 045.211	1.591	100:0
	0.28		10740 ± 120	10886.384	0.315	100:0
				11 049.202	2.619	100:0
$J = 1$	0.33			10 905.503	0.322	100:0
	0.23			10 905.552	0.319	38.805:61.195
				11 008.389	0.432	61.252:38.748
	0.28	10730 ± 100	-	10 922.365	0.325	38.431:61.569
$J = 2$				11 013.321	0.451	61.637:38.364
	0.33			10 938.010	0.333	38.040:61.960
				11 018.666	0.477	62.061:37.939
	0.23			10 837.374	0.296	24.262:75.738
$J = 2$				11 014.714	0.409	76.721:23.279
	0.28		-	10 860.999	0.302	24.262:75.738
				11 020.364	0.426	76.720:23.280
	0.33			10 882.462	0.308	24.276:75.724
			11 026.391	0.452	76.828:23.172	

B. Bottom analog Z_{bb}^+

The bottom analog Z_{bb}^+ denotes the state obtained by replacing both the charm quark and antiquark in $Z^+(4430)$ with a bottom quark and antiquark. Although the masses of P wave B mesons B_2, B_1, B'_1 , and B_0 are very close to each other [36,54], the widths of B'_1 and B_0 are very large. Therefore, we shall only include $B^*\bar{B}_1$ and $B^*\bar{B}_2$ in our coupled channel analysis analogous to the $Z^+(4430)$ case. The matrix elements of the residual interaction V_I have features similar to the $D^*\bar{D}_1$ and $D^*\bar{D}_2$ systems except that the former is larger than the latter in magnitude. Furthermore, since the kinetic energy is greatly reduced compared with the charmed system, Z_{bb}^+ should be more strongly bound than $Z^+(4430)$. The numerical results are

shown in Table IV. It is obvious that bound state solutions with $J^P = 0^-, 1^-,$ and 2^- can be found. The smaller kinetic energy and deeper potential lead to two eigenstates. The first states are tightly bound with the binding energy from 120 to 200 GeV. The binding energy of the second bound states with $J^P = 1^-$ and 2^- is in the range of 20 to 40 GeV, and the $B^*\bar{B}_1$ component dominates over $B^*\bar{B}_2$. While the second state with $J^P = 0^-$ is loosely bound, it disappears for $\mu = 0.33$ GeV. The masses predicted from the potential model [7] and QCD sum rule [10] are shown as well. Our results are consistent with these predictions within theoretical errors. The corresponding eigenstate wavefunctions with $\mu = 0.28$ GeV are displayed in Fig. 5. It is remarkable that the bound state solutions

 TABLE V. The predictions for the mass, the rms and the ratio between different components of Z_{bc}^{++} . The mass prediction in Ref. [7] is also listed.

	μ	Mass (MeV) in [7]	Mass (MeV)	rms (fm)	$P(D^*B_1) : P(D^*B_2) : P(D_1B^*) : P(D_2B^*)$
$J = 0$	0.23		7659.800	0.540	81.453:0:18.547:0
	0.28		7672.663	0.569	84.253:0:15.747:0
	0.33		7683.562	0.605	86.883:0:13.117:0
	0.23		7625.797	0.447	35.938:15.897:17.609:30.556
$J = 1$			7699.090	0.640	31.107:58.512:7.668:2.713
	0.28	7630 ± 100	7642.649	0.461	36.791:15.586:17.048:30.575
			7707.872	0.692	32.246:59.236:6.727:1.791
	0.33		7657.519	0.477	37.799:15.270:16.504:30.426
$J = 2$			7715.295	0.766	33.693:59.341:5.924:1.042
	0.23		7628.911	0.450	0.290:38.295:39.540:21.875
			7720.202	0.921	76.568:0.102:10.625:12.704
	0.28		7646.478	0.464	0.214:37.210:40.796:21.779
			7729.487	1.853	88.240:0.039:5.549:6.173
	0.33		7661.866	0.480	0.154:36.092:42.079:21.675

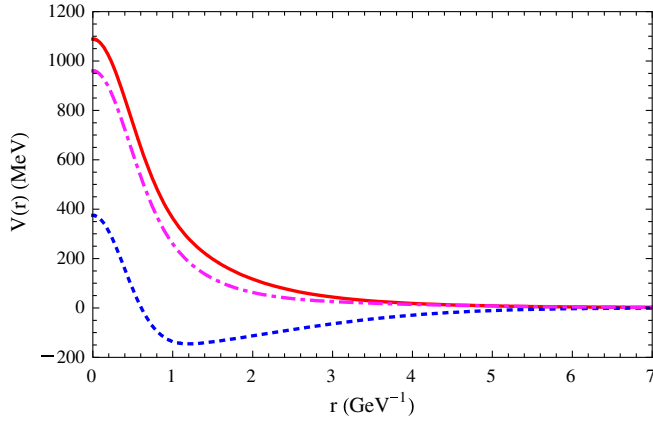


FIG. 4 (color online). The potentials for the $I = 0$ DD^* system. The short-dashed line represents the nondiagonal potential $V_{12}(r)$, the solid and dashed-dotted lines, respectively, denote the diagonal potential $V_{11}(r)$ and $V_{22}(r)$.

predicted in our model are drastically different from those of the π and σ exchange model in the heavy quark effective theory, where only the $0^- B^* \bar{B}_1$ molecule is allowed to exist [16]. Therefore, the experimental search for the bottom analog Z_{bb}^+ is of great interest to distinguish the different mechanisms in generating the molecular states.

Clearly, the analogous state Z_{bb}^+ should be searched for in the $\Upsilon(2S)\pi^+$ channel, where $\Upsilon(2S)$ can be detected by

its decay into $\Upsilon(1S)\pi\pi$. Because of its large mass, at present the most promising place to produce Z_{bb}^+ conspicuously is the large hadron colliders such as Tevatron and LHC. If its spin parity is $J^P = 1^-$, its neutral partner Z_{bb}^0 is $J^{PC} = 1^{--}$, then we can search for Z_{bb}^0 via e^+e^- annihilation at B factory.

C. Double charged states Z_{bc}^{++}

The state Z_{bc}^{++} is obtained by replacing the charm antiquark in $Z^+(4430)$ with a bottom antiquark, which carry a two unit electric charge. The state replacing the charm quark with the bottom quark is conjugated to Z_{bc}^{++} , and the static properties such as mass, rms, etc. are the same as those of Z_{bc}^{++} . Consequently, we only need to discuss one of them, where we focus on Z_{bc}^{++} . The analysis is somewhat different from $Z^+(4430)$ and Z_{bb}^+ , because the masses of D^*B_1 , D^*B_2 , D_1B^* , and D_2B^* are almost degenerate, we should solve the four channels coupled Schrödinger equation instead of the two channels coupled equation. Since the total angular momentum of the S wave D^*B_2 and D_2B^* cannot be zero, the four channel coupled Schrödinger equation is reduced to two channel coupled Schrödinger equations for the $J^P = 0^-$ state. The numerical results for the lowest states are given in Table V. For $J^P = 1^-$ and 2^- , the second bound state can appear for appropriate μ values. The binding energies of the first bound state are in the

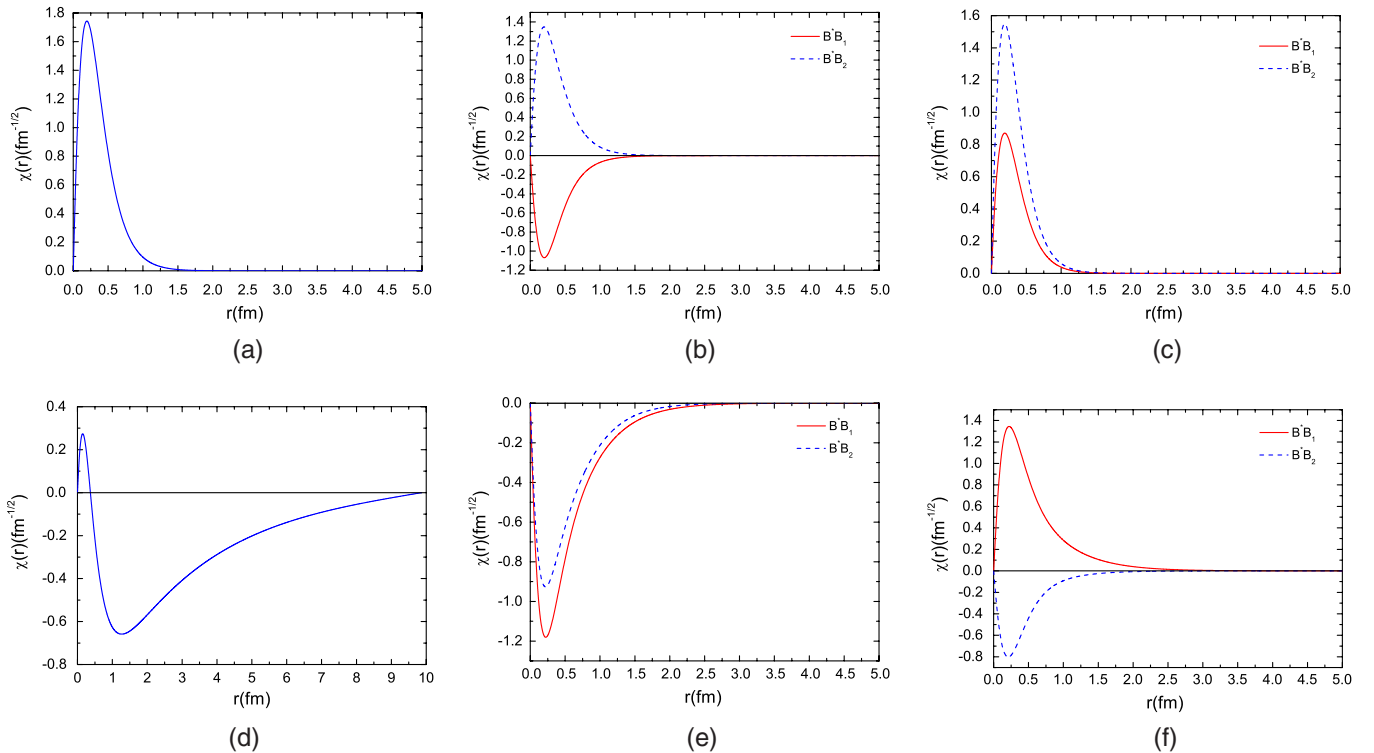


FIG. 5 (color online). The radial wave functions $\chi(r) = rR(r)$ for Z_{bb}^+ , (a), (b), and (c) are, respectively, the wavefunctions of the first bound states with $J^P = 0^-$, $J^P = 1^-$, and $J^P = 2^-$, and (d), (e), and (f) are the second state wavefunctions.

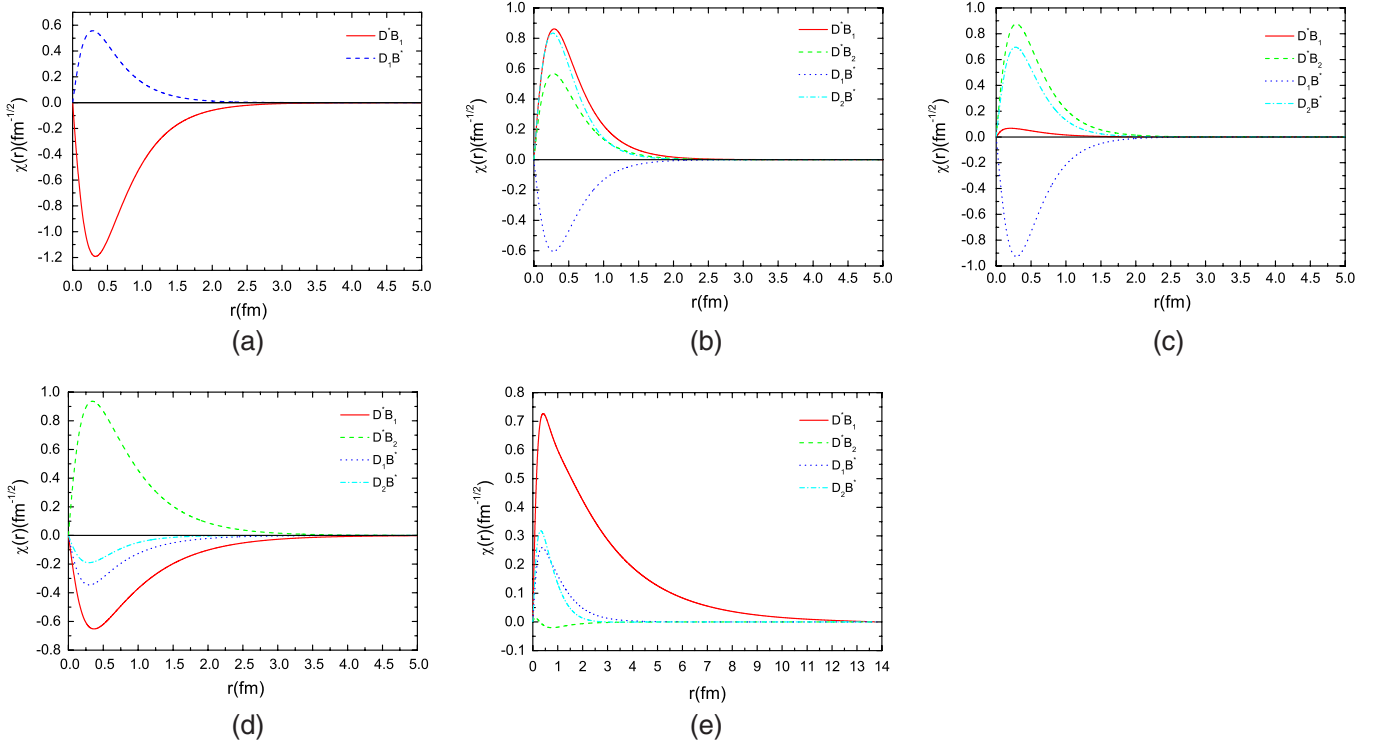


FIG. 6 (color online). The radial wave functions $\chi(r) = rR(r)$ of Z_{bc}^{++} , (a), (b), and (c) are, respectively, the wavefunctions of the first bound states with $J^P = 0^-$, $J^P = 1^-$, and $J^P = 2^-$, and (d) and (e) are the second state wavefunctions with $J^P = 1^-$ and $J^P = 2^-$, respectively.

range of 70 to 100 MeV, which are larger than the binding energy of the $D^*\bar{D}_1$ system and smaller than those of Z_{bb}^+ . A similar pattern has been found for the second bound state solution when it exists. The mass predicted in Ref. [7] from potential model is shown as well and is in agreement with our results within the theoretical errors. We plot the eigenstate wavefunctions in Fig. 6. This state is difficult to be produced, since both the charm quark and bottom quark have to be produced simultaneously. The direct production of this state at hadron colliders, such as LHC and Tevatron, is most promising, and we could search for Z_{bc}^{++} via the decay channel $Z_{bc}^{++} \rightarrow B_c^+(2S)\pi^+$. If the double charged state Z_{bc}^{++} is observed in the future, it would be unambiguously exotic states beyond the quark model, and it would be a great support to the hadronic molecule picture.

D. DD^* system

The S wave DD^* system with zero isospin will couple with D^*D^* under the residual interactions in Eq. (5) and (9), which is governed by the spin-spin interaction. In the heavy quark limit, the effective potentials are induced by the interactions between two light antiquarks, which is repulsive. The effective potentials for $\mu = 0.28$ GeV are illustrated in Fig. 4. It is obvious that the diagonal components of the effective potentials are really repulsive, and the off-diagonal potential is smaller than the diagonal components. Numerically solving the two chan-

nel coupled Schrödinger equation, we do not find bound state solutions. The attractive interaction is so weak that DD^* bound states do not exist. The same conclusion has been reached from the one boson exchange model [52].

VI. SUMMARY AND DISCUSSIONS

We have dynamically studied $Z^+(4430)$ and analogous heavy flavor states in the quark model. The proximity of $Z^+(4430)$ to the $D^*\bar{D}_1$ threshold strongly suggests that it may be a molecular state. For a loosely bound molecule, the interaction between the constituents of the interacting hadrons occurs at a relatively large separation. As a consequence, the interaction will be subject to screening due to the production of dynamical quark and gluon. The effective charge turns out to properly describe the interactions between the constituents of the two hadrons at a large distance, which is incorporated in this work. Because the spin-spin interaction is known to be important in the nonrelativistic quark models, we have included the spin-spin interaction in addition to the screened color Coulomb and screened linear confinement interactions in our model.

The residual interactions between two hadrons induce a state mixing effect, which is taken into account by solving the coupled channel Schrödinger equation numerically, where the second order perturbation theory cannot be used anymore. We have focused on the nearly degenerate channels, which is a good approximation. The numerical

calculations are performed with the help of the MATSCS and FESSDE2.2 packages, and the results obtained by the two packages are the same within error.

For the $D^*\bar{D}_1$ system coupled with $D^*\bar{D}_2$, $J^P = 0^-$, and 2^- bound states exist for reasonable parameter values. However, the $J^P = 1^-$ bound state solution can be found only if the screening mass μ is smaller than 0.16 GeV. We suggest that the most favorable quantum is 0^- , if $Z^+(4430)$ is confirmed to be a loosely bound state by future experiments. More precise measurements of $Z^+(4430)$ mass and width, partial wave analysis are helpful to understand its nature. If partial wave analysis favors the quantum number 0^- or 2^- , it would strongly support the hypothesis of $Z^+(4430)$ as a molecular state. Before concluding that $Z^+(4430)$ is a $D^*\bar{D}_1$ molecule unambiguously, we should further study the decay and production properties under the hadronic molecule ansatz, then compare the theoretical predictions with experimental data. In addition, other effects such as cusp [14], etc. should be taken into account, which is beyond the scope of the present work [55].

The bottom analog Z_{bb}^+ and Z_{bc}^{++} are considered as well. The former is obtained by replacing both the charm quark and antiquark in $Z^+(4430)$ with bottom the quark and antiquark, and the latter by replacing the charm antiquark with the bottom antiquark. The second bound state may appear because of the smaller kinetic energy and deeper potential. The masses predicted in our model are in agreement with predictions from the potential model [7] and the QCD sum rule [10]. We suggest searching for these states at Tevatron and LHC via $Z_{bb}^+ \rightarrow Y(2S)\pi^+$ and $Z_{bc}^{++} \rightarrow B_c^+(2S)\pi^+$, respectively.

We have applied our model to $D\bar{D}^*$ and DD^* systems as well. The 1^{++} $D\bar{D}^*$ bound state solution coupled with $D_1\bar{D}_2$ can be found only if the screening mass μ is smaller than 0.17 GeV. The mixing between the molecular state and the conventional charmonium should be considered to understand the nature of $X(3872)$. For the exotic DD^* system, the diagonal components of the effective potentials are repulsive, and the magnitude of the off-diagonal potentials are not attractive enough to lead to bound states.

Our model is different from the one boson exchange model and other hadronic molecule models [16,20,21,52]; consequently, the predicted bound state solutions are drastically different from each other. We suggest that the search

for the bottom analog Z_{bb}^+ is crucial in distinguishing the different models.

In this work, we have studied the $(Q\bar{q})-(q\bar{Q})$ system, where Q denotes the heavy quark and q represents the light quark. Under short distance interactions, such as the one-gluon exchange induced constituent quark interchange interactions [35], the $(Q\bar{q})-(q\bar{Q})$ configuration may mix with the $(Q\bar{Q})-(q\bar{q})$ configuration. In Ref. [21], Swanson considered both the long distance one-pion exchange and the short distance quark interchange interactions. He found that the probability of the mixing of $J/\psi\omega$ with $D\bar{D}^*$ ranges from zero to a maximum mixing of 17%. For the heavy flavor systems considered in the present work, the mass difference between $(Q\bar{q})-(q\bar{Q})$ and $(Q\bar{Q})-(q\bar{q})$ is larger than that in Ref. [21]; therefore, the mixing between the two configurations should be smaller. We expect that this mixing effect plays a minor role in the systems considered above.

The discovery of the $Y(4260)$ and $Y(4360)$ represents an overpopulation of the expected 1^{--} charmonium states. As is suggested in Refs. [56–59], a possible way of reconciling $Y(4260)$ and $Y(4360)$ is as follows: $Y(4260)$ is a $D\bar{D}_1$ molecule, whereas $Y(4360)$ is a charmonium hybrid. It is interesting to investigate whether the $D\bar{D}_1$ system admits a 1^{--} molecular state with mass of about 4260 MeV along the same line.

ACKNOWLEDGMENTS

We acknowledge Professor Dao-Neng Gao and Professor Qiang Zhao for very helpful and stimulating discussions, and we are grateful to Dr. Jian Deng and Professor V. Ledoux for their help on numerical calculations. This work is supported by National Natural Science Foundation of China under Grant No. 90403021 and China Postdoctoral Science Foundation Grant No. 20070420735. Jia-Feng Liu is supported in part by the National Natural Science Foundation of China under Grant No. 10775124.

APPENDIX A: THE SPATIAL MATRIX ELEMENTS INVOLVED IN THE WORK

Firstly we give the matrix elements of screened color Coulomb, screened linear confinement, and spin-spin hyperfine interactions between the ground states

$$\begin{aligned}
 V_{00}^{(1)}(ij, r) &\equiv \langle 0, 0; 0, 0 | V_r^{(1)}(\mathbf{r}_{ij}) | 0, 0; 0, 0 \rangle = e^{a_{ij}^2 \mu^2} \frac{\alpha_s}{2r} \left\{ e^{-\mu r} \left[1 + \text{Erf} \left(\frac{r}{2a_{ij}} - \mu a_{ij} \right) \right] - e^{\mu r} \left[1 - \text{Erf} \left(\frac{r}{2a_{ij}} + \mu a_{ij} \right) \right] \right\} \\
 V_{00}^{(2)}(ij, r) &\equiv \langle 0, 0; 0, 0 | V_r^{(2)}(\mathbf{r}_{ij}) | 0, 0; 0, 0 \rangle = e^{a_{ij}^2 \mu^2} \frac{3b}{8\mu r} \left\{ (r - 2\mu a_{ij}^2) e^{-\mu r} \left[1 + \text{Erf} \left(\frac{r}{2a_{ij}} - \mu a_{ij} \right) \right] \right. \\
 &\quad \left. + (r + 2\mu a_{ij}^2) e^{\mu r} \left[1 - \text{Erf} \left(\frac{r}{2a_{ij}} + \mu a_{ij} \right) \right] \right\} \\
 V_{00}^{(3)}(ij, r) &\equiv \langle 0, 0; 0, 0 | V_r^{(3)}(\mathbf{r}_{ij}) | 0, 0; 0, 0 \rangle = -\frac{\alpha_s}{3\pi^{1/2} m_i m_j a_{ij}^3} e^{-(r^2/4a_{ij}^2)},
 \end{aligned} \tag{A1}$$

where $a_{ij} = \sqrt{\frac{f_A^2(ij)}{4\beta_A^2} + \frac{f_B^2(ij)}{4\beta_B^2}}$, β_A and β_B are, respectively, the harmonic oscillator parameters of the A meson and B meson. $\text{Erf}(x)$ is the error function $\text{Erf}(x) = \frac{2}{\sqrt{\pi}} \int_0^x e^{-t^2} dt$. Other matrix elements can be expressed in terms of the derivative of $V_{00}^{(k)}(ij, r)$ with respect to r . Concretely they are given as follows:

$$\begin{aligned}
 \langle 1, 1; 1, -1 | V_r^{(k)}(\mathbf{r}_{ij}) | 0, 0; 0, 0 \rangle &= \frac{f_A(ij)f_B(ij)}{2\beta_A\beta_B} \frac{1}{r} \frac{\partial}{\partial r} V_{00}^{(k)}(ij, r) & \langle 1, 0; 1, 0 | V_r^{(k)}(\mathbf{r}_{ij}) | 0, 0; 0, 0 \rangle &= -\frac{f_A(ij)f_B(ij)}{2\beta_A\beta_B} \frac{\partial^2}{\partial r^2} V_{00}^{(k)}(ij, r) \\
 \langle 1, -1; 1, 1 | V_r^{(k)}(\mathbf{r}_{ij}) | 0, 0; 0, 0 \rangle &= \frac{f_A(ij)f_B(ij)}{2\beta_A\beta_B} \frac{1}{r} \frac{\partial}{\partial r} V_{00}^{(k)}(ij, r) & \langle 0, 0; 1, 1 | V_r^{(k)}(\mathbf{r}_{ij}) | 0, 0; 1, 1 \rangle &= \left[1 + \frac{f_B^2(ij)}{2\beta_B^2} \frac{1}{r} \frac{\partial}{\partial r} \right] V_{00}^{(k)}(ij, r) \\
 \langle 1, 1; 0, 0 | V_r^{(k)}(\mathbf{r}_{ij}) | 0, 0; 1, 1 \rangle &= \frac{f_A(ij)f_B(ij)}{2\beta_A\beta_B} \frac{1}{r} \frac{\partial}{\partial r} V_{00}^{(k)}(ij, r) & \langle 0, 0; 1, 0 | V_r^{(k)}(\mathbf{r}_{ij}) | 0, 0; 1, 0 \rangle &= \left[1 + \frac{f_B^2(ij)}{2\beta_B^2} \frac{\partial^2}{\partial r^2} \right] V_{00}^{(k)}(ij, r) \\
 \langle 1, 0; 0, 0 | V_r^{(k)}(\mathbf{r}_{ij}) | 0, 0; 1, 0 \rangle &= \frac{f_A(ij)f_B(ij)}{2\beta_A\beta_B} \frac{\partial^2}{\partial r^2} V_{00}^{(k)}(ij, r) & \langle 0, 0; 1, -1 | V_r^{(k)}(\mathbf{r}_{ij}) | 0, 0; 1, -1 \rangle &= \left[1 + \frac{f_B^2(ij)}{2\beta_B^2} \frac{1}{r} \frac{\partial}{\partial r} \right] V_{00}^{(k)}(ij, r) \\
 \langle 1, -1; 0, 0 | V_r^{(k)}(\mathbf{r}_{ij}) | 0, 0; 1, -1 \rangle &= \frac{f_A(ij)f_B(ij)}{2\beta_A\beta_B} \frac{1}{r} \frac{\partial}{\partial r} V_{00}^{(k)}(ij, r) & \langle 0, 0; 1, 1 | V_r^{(k)}(\mathbf{r}_{ij}) | 1, 1; 0, 0 \rangle &= \frac{f_A(ij)f_B(ij)}{2\beta_A\beta_B} \frac{1}{r} \frac{\partial}{\partial r} V_{00}^{(k)}(ij, r) \\
 \langle 1, 1; 0, 0 | V_r^{(k)}(\mathbf{r}_{ij}) | 1, 1; 0, 0 \rangle &= \left[1 + \frac{f_A^2(ij)}{2\beta_A^2} \frac{1}{r} \frac{\partial}{\partial r} \right] V_{00}^{(k)}(ij, r) & \langle 0, 0; 1, 0 | V_r^{(k)}(\mathbf{r}_{ij}) | 1, 0; 0, 0 \rangle &= \frac{f_A(ij)f_B(ij)}{2\beta_A\beta_B} \frac{\partial^2}{\partial r^2} V_{00}^{(k)}(ij, r) \\
 \langle 1, 0; 0, 0 | V_r^{(k)}(\mathbf{r}_{ij}) | 1, 0; 0, 0 \rangle &= \left[1 + \frac{f_A^2(ij)}{2\beta_A^2} \frac{\partial^2}{\partial r^2} \right] V_{00}^{(k)}(ij, r) & & \\
 \langle 0, 0; 1, -1 | V_r^{(k)}(\mathbf{r}_{ij}) | 1, -1; 0, 0 \rangle &= \frac{f_A(jk)f_B(jk)}{2\beta_A\beta_B} \frac{1}{r} \frac{\partial}{\partial r} V_{00}^{(k)}(ij, r) & \langle 1, -1; 0, 0 | V_r^{(k)}(\mathbf{r}_{ij}) | 1, -1; 0, 0 \rangle &= \left[1 + \frac{f_A^2(jk)}{2\beta_A^2} \frac{1}{r} \frac{\partial}{\partial r} \right] V_{00}^{(k)}(ij, r).
 \end{aligned} \tag{A2}$$

-
- [1] S.-K. Choi *et al.* (Belle Collaboration), Phys. Rev. Lett. **100**, 142001 (2008).
- [2] B. Aubert, *et al.* (BABAR Collaboration), arXiv:0811.0564.
- [3] G. J. Ding, arXiv:0711.1485.
- [4] J. L. Rosner, Phys. Rev. D **76**, 114002 (2007).
- [5] L. Maiani, A. D. Polosa, and V. Riquer, arXiv:0708.3997.
- [6] C. Meng and K. T. Chao, arXiv:0708.4222.
- [7] K. m. Cheung, W. Y. Keung, and T. C. Yuan, Phys. Rev. D **76**, 117501 (2007).
- [8] S. S. Gershtein, A. K. Likhoded, and G. P. Pronko, arXiv:0709.2058.
- [9] C. F. Qiao, J. Phys. G **35**, 075008 (2008).
- [10] S. H. Lee, A. Mihara, F. S. Navarra, and M. Nielsen, Phys. Lett. B **661**, 28 (2008).
- [11] X. Liu, Y. R. Liu, W. Z. Deng, and S. L. Zhu, Phys. Rev. D **77**, 034003 (2008).
- [12] Y. Li, C. D. Lu, and W. Wang, Phys. Rev. D **77**, 054001 (2008).
- [13] E. Braaten and M. Lu, arXiv:0712.3885.
- [14] D. V. Bugg, J. Phys. G **35**, 075005 (2008); arXiv:0806.3566.
- [15] X. H. Liu, Q. Zhao, and F. E. Close, Phys. Rev. D **77**, 094005 (2008).
- [16] X. Liu, Y. R. Liu, W. Z. Deng, and S. L. Zhu, Phys. Rev. D **77**, 094015 (2008).
- [17] X. Liu, B. Zhang, and S. L. Zhu, Phys. Rev. D **77**, 114021 (2008).
- [18] M. Cardoso and P. Bicudo, arXiv:0805.2260.
- [19] M. B. Voloshin and L. B. Okun, Pis'ma Zh. Eksp. Teor. Fiz. **23**, 369 (1976); [JETP Lett. **23**, 333 (1976)]; A. De Rujula, H. Georgi, and S. L. Glashow, Phys. Rev. Lett. **38**, 317 (1977).
- [20] N. A. Tornqvist, Phys. Rev. Lett. **67**, 556 (1991); Z. Phys. C **61**, 525 (1994).
- [21] E. S. Swanson, Phys. Lett. B **588**, 189 (2004); Phys. Rep. **429**, 243 (2006).
- [22] A. De Rujula, H. Georgi, and S. L. Glashow, Phys. Rev. D **12**, 147 (1975).
- [23] S. Godfrey and N. Isgur, Phys. Rev. D **32**, 189 (1985).
- [24] T. Appelquist, M. Dine, and I. J. Muzinich, Phys. Rev. D **17**, 2074 (1978).
- [25] M. E. Peskin, Nucl. Phys. **B156**, 365 (1979); G. Bhanot and M. E. Peskin, Nucl. Phys. **B156**, 391 (1979); G. Bhanot, W. Fischler, and S. Rudaz, Nucl. Phys. **B155**, 208 (1979).
- [26] C. Y. Wong, Phys. Rev. C **69**, 055202 (2004).
- [27] G. S. Bali, Phys. Rev. D **62**, 114503 (2000).
- [28] H. J. Lipkin, Phys. Lett. **113B**, 490 (1982).
- [29] W. N. Zhang and C. Y. Wong, Phys. Rev. C **68**, 035211

- (2003).
- [30] T. Barnes and E. S. Swanson, Phys. Rev. D **46**, 131 (1992).
- [31] T. Barnes, N. Black, D. J. Dean, and E. S. Swanson, Phys. Rev. C **60**, 045202 (1999).
- [32] C. Y. Wong, E. S. Swanson, and T. Barnes, Phys. Rev. C **65**, 014903 (2001); **66**, 029901(E) (2002).
- [33] N. R. Walet and R. D. Amado, Phys. Rev. C **47**, 498 (1993).
- [34] G. J. Ding and M. L. Yan, Phys. Rev. C **75**, 034004 (2007).
- [35] E. S. Swanson, Ann. Phys. (N.Y.) **220**, 73 (1992).
- [36] C. Amsler *et al.* (Particle Data Group), Phys. Lett. B **667**, 1 (2008).
- [37] C. Y. Wong, Phys. Rev. D **60**, 114025 (1999).
- [38] E. S. Ackleh, T. Barnes, and E. S. Swanson, Phys. Rev. D **54**, 6811 (1996).
- [39] S. Capstick and W. Roberts, Phys. Rev. D **49**, 4570 (1994).
- [40] S. Godfrey and R. Kokoski, Phys. Rev. D **43**, 1679 (1991).
- [41] V. Ledoux, M. Van Daele, and G. Vanden Berghe, Comput. Phys. Commun. **176**, 191 (2007).
- [42] A. G. Abrashkevich, D. G. Abrashkevich, M. S. Kaschiev, and I. V. Puzynin, Comput. Phys. Commun. **85**, 40 (1995); **85**, 65 (1995); **115**, 90 (1998).
- [43] S. K. Choi *et al.* (Belle Collaboration), Phys. Rev. Lett. **91**, 262001 (2003).
- [44] D. E. Acosta *et al.* (CDF II Collaboration), Phys. Rev. Lett. **93**, 072001 (2004).
- [45] V. M. Abazov *et al.* (D0 Collaboration), Phys. Rev. Lett. **93**, 162002 (2004).
- [46] B. Aubert *et al.* (BABAR Collaboration), Phys. Rev. D **71**, 071103 (2005).
- [47] A. Abulencia *et al.* (CDF Collaboration), Phys. Rev. Lett. **98**, 132002 (2007).
- [48] N. A. Tornqvist, Phys. Lett. B **590**, 209 (2004); F. E. Close and P. R. Page, Phys. Lett. B **578**, 119 (2004); C. Y. Wong, Phys. Rev. C **69**, 055202 (2004); E. S. Swanson, Phys. Lett. B **588**, 189 (2004).
- [49] M. Suzuki, Phys. Rev. D **72**, 114013 (2005).
- [50] Y. R. Liu, X. Liu, W. Z. Deng, and S. L. Zhu, Eur. Phys. J. C **56**, 63 (2008).
- [51] C. E. Thomas and F. E. Close, Phys. Rev. D **78**, 034007 (2008).
- [52] G. J. Ding, J. F. Liu, and M. L. Yan, arXiv:0901.0426.
- [53] B. Fulsom *et al.* (BABAR Collaboration), arXiv:0809.0042.
- [54] A. Gessler (CDF Collaboration), J. Phys. Conf. Ser. **110** 022011 (2008).
- [55] (work in progress).
- [56] G. J. Ding, J. J. Zhu, and M. L. Yan, Phys. Rev. D **77**, 014033 (2008).
- [57] G. J. Ding, Phys. Rev. D **79**, 014001 (2009).
- [58] E. Swanson, AIP Conf. Proc. **814**, 203 (2006); Int. J. Mod. Phys. A **21**, 733 (2006).
- [59] F. E. Close, arXiv:0801.2646; in Proceedings of the 5th Flavor Physics and CP Violation Conference (FPCP 2007), Bled, Slovenia, 2007, p. 020 (unpublished).